energy differences between structural alternatives become smaller but the shape of the energy difference curves become closer to those of **3**. Thus, in the fluorides there is the very real possibility that the overall picture is a balance between "local" and "extended" effects. There is some experimental evidence that points toward this state of affairs. It is interesting to note that a distortion of type **1** is found very strongly for FeF_2, a configuration where the energy is lowered on distortion by both local and extended mechanisms, but a much smaller effect is seen in CoF_2, where the local mechanism favors **2** but the extended mechanism favors **1**.

We can also see which distortion of the octahedron is predicted from the ionic model. Instead of performing Madelung calculations with the lack of insight that the computed numbers give us, we will use an idea of O'Keeffe.[34] He suggested that the lowest energy structure is the one of *maximum* volume, subject to the constraint of a fixed anion–cation distance, since here the anion–anion repulsions should be minimized. (Such a model naturally ignores the other terms in the energy, such as the cation–cation interactions.) In terms of the two distances around the metal atom the volume of the unit cell is given by eq 2. The

$$V^2 = (r_2^4/u^6)[r_4^2u^2 - (\tfrac{1}{2} - u)^2r_2^2] \qquad (2)$$

change in this value on stretching r_2 and compressing r_4 in the way indicated in eq 1 is proportional to eq 3, which is positive if $u > 0.25$. This result is of course similar to the one we obtained

$$u^2 - (\tfrac{1}{2} - u)^2 \qquad (3)$$

earlier for TiO_2, namely that the relief of anion–anion repulsions (whether of the ionic or covalent type) is best achieved in the 2L + 4S mode. An ionic model then encourages distortion in the opposite direction to that actually observed.

This experimental observation of the titanium atom "rattling" in the hole in the rutile structure indicates that the Ti–O distance should be somewhat shorter if anion–cation forces dominated the picture. It also leads us to ask whether tetrahedral coordination should be favored. The answer, difficult to quantify is that, for this d^0 metal, π bonding with the metal is especially good in the octahedral geometry.

The ideas described in this work have used one-electron molecular orbital theory. The crystal field theory has also been used to study molecular problems of this type.[35] Certainly, since the form of the splitting patterns of octahedral transition-metal energy levels are controlled purely by symmetry, the crystal field predictions as to the preferred route for these molecules will be similar to those obtained with the angular overlap model, although the distinction between π donors and acceptors does not exist on the crystal field model. In the extended solid the result we have shown in **5** involving mixing of the a_1 orbitals may be mimicked by the addition of a uniaxial field of judiciously chosen strength along the chain direction. We prefer to describe this structural problem by using the language of the covalent angular overlap model with its quantitative aspects associated with σ and π strengths rather than the comparatively vague ideas of the crystal field theory.

Acknowledgment. This research was supported by the National Science Foundation, by Grant (to J.K.B.) NSF DMR8414175, and by a grant through the Materials Research Laboratory at the University of Chicago (NSF DMR8519460). J.W.R. acknowledges support of the Intense Pulsed Neutron Source by DOE, Contract W-31-109-ENG-38. We thank J. D. Jorgensen and K. J. Volin of Argonne National Laboratory for use of the SEPD diffractometer and Dr. R. Kulkarni for performing some of the calculations. We are extremely grateful to Dr. Arthur Sleight and his group at Du Pont for the gift of a sample of CrO_2.

Appendix

The tight-binding calculations were performed along the lines of the earlier work[15] and with the same parameters for metal and oxygen. The parameters for fluorine were however (exponents in parentheses) the following: 2s, $H_{ii} = -40.00$ eV (1.245); 2p, $H_{2i} = -30.00$ eV (1.245).

Registry No. CrO_2, 12018-01-8.

Supplementary Material Available: Tables of time-of-flight and *d* spacing for CrO_2 at room temperature and 173 and 10 K (33 pages). Ordering information is given on any current masthead page.

---

(34) O'Keeffe, M. *Acta. Crystallogr.* **1977**, *A33*, 924.

(35) *Dunn*, T. M.; McClure, D. S.; Pearson, R. G. *Some Aspects of Crystal Field Theory*; Harper and Row: New York, 1965.

Vanadium Nitride Linear Chain Polymers and Monomers. Synthesis and Structures of $[V(\mu\text{-}N)Cl_2(py)_2]_\infty$ and $V(N)Cl_2(quin)_2$

Susan C. Critchlow, Megan E. Lerchen, Randal C. Smith, and Nancy M. Doherty*

Contribution from the Department of Chemistry, University of Washington, Seattle, Washington 98195. *Received November 20, 1987. Revised Manuscript Received June 2, 1988*

Abstract: A series of vanadium(V) nitrido complexes of formula $[V(N)Cl_2L_2]_n$ has been prepared by net loss of chlorotrimethylsilane from the vanadium(V) trimethylsilylimido trichloride, $Cl_3V{\equiv}NSiMe_3$, on reaction with substituted pyridines or an amine. For L = py or 4-Mepy, insoluble nitride-bridged linear chain polymers are produced. An X-ray structure of $[V(\mu\text{-}N)Cl_2(py)_2]_\infty$ reveals distorted octahedral vanadium centers joined by alternating short (1.571 (7) Å) and long (2.729 (7) Å) V–N bonds. In contrast, for L = 4-Etpy, 4-*t*-Bupy, or quinuclidine, soluble monomeric terminal nitride complexes are formed. The X-ray structure of $V(N)Cl_2(quin)_2$ indicates that this compound also possesses a monomeric five-coordinate structure in the solid state with a short (1.568 (19) Å) terminal metal nitride bond. The stability of the nitride bridge is discussed in light of the differences in structure and solubility in this group of compounds and in terms of the observed interactions involving the ancillary ligands in the solid-state structure of $[V(\mu\text{-}N)Cl_2(py)_2]_\infty$.

The development of synthetic routes to transition-metal-containing polymers is a critical prerequisite for study of these important new materials.[1-3] We are particularly interested in polymers based on a metal–nitrogen backbone, $[M(\mu\text{-}N)L_n]_\infty$.

0002-7863/88/1510-8071\$01.50/0

Transition-metal nitrido complexes which adopt polymeric structures in the solid state are known;[4,5] however, there are no general methods for preparing such materials. Additionally, the nitride bridges in the known compounds are quite labile, as demonstrated by their cleavage by added ligands[4] and by their dissolution in aromatic solvents producing monomeric species.[5]

We have been exploring the condensation reaction shown in eq 1 as a route to heterobimetallic μ-nitride derivatives possessing robust metal–nitrogen bonds (eq 1, X = F or Cl).[6] When the

$$L_nM(NSiMe_3) + XM'L'_n \xrightarrow{-XSiMe_3} L_nM(\mu\text{-}N)M'L'_n \quad (1)$$

starting trimethylsilylimido compound also possesses a reactive halide ligand, preparation of polymeric metal nitrides should be possible. We report here the use of this condensation reaction for the synthesis of vanadium nitride linear chain polymers and related monomers and discuss the influence of the coordinated ligands on the stability and structure of the nitride bridge.

Results

A vanadium(V) derivative having both silylimido and halide ligands, $Cl_3V{\equiv}NSiMe_3$ (**1**), is readily prepared by a ligand exchange between $(Me_3SiO)_3V{\equiv}NSiMe_3$[7] and 3.5 equiv of $Cl_3V{\equiv}O$ in pentane at −78 °C.[8] Orange **1**, which crystallizes from the reaction mixture at −78 °C, is collected by removal of the supernatant liquid and purified by Kugelrohr sublimation at 30 °C. An alternative synthesis of **1** by the reaction of VCl_4 with 2 equiv of Me_3SiN_3 has been described by Dehnicke and co-workers.[9] Compound **1** is extremely air and water sensitive, it is very volatile, and it decomposes at ambient temperatures both in solution and in the solid state.

Addition of 2 or more equiv of pyridine to a solution of **1** in benzene results in immediate formation of a pink precipitate, $[V(\mu\text{-}N)Cl_2(py)_2]_\infty$ (**2a**), in quantitative yield with loss of 1 equiv of chlorotrimethylsilane (eq 2). Compound **2a** is also formed

$$\begin{array}{ccl} Cl_3V{\equiv}NSiMe_3 + 2L & \xrightarrow{-ClSiMe_3} & [V(\mu\text{-}N)Cl_2L_2]_\infty \quad (2) \\ \mathbf{1} & & \mathbf{2a},\ L = py \\ & & \mathbf{2b},\ L = 4\text{-}Mepy \end{array}$$

in methylene chloride solution or by the reaction of **1** with neat pyridine. The IR spectrum of this compound shows a strong band at 968 cm^{-1} which can be assigned to a V≡N stretch,[10,11] in addition to bands characteristic of coordinated pyridine.[12] This material is completely insoluble at ambient temperatures in all solvents with which it does not react and decomposes at elevated temperatures in pyridine. Despite accompanying decomposition, X-ray quality crystals can be obtained as red needles by dissolution of **2a** in pyridine at 120 °C followed by immediate cooling.

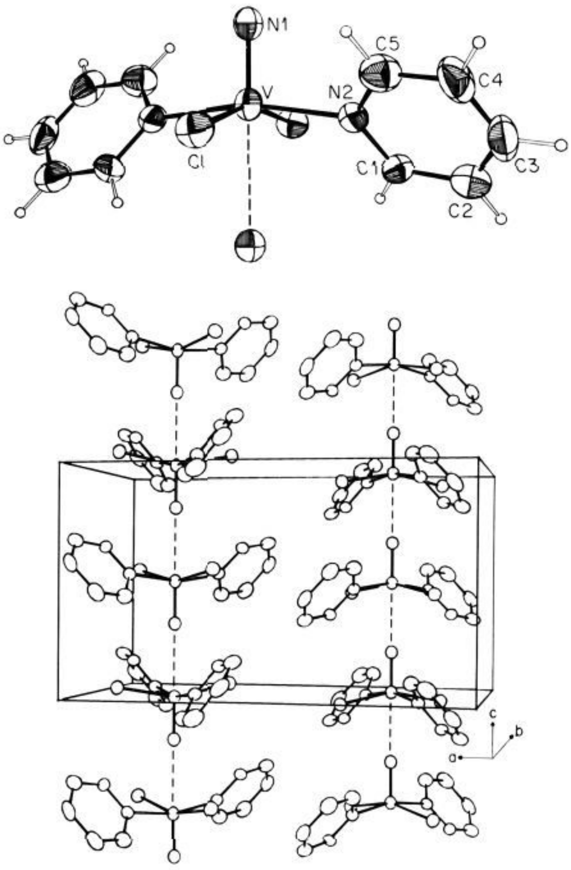

Figure 1. ORTEP drawings of $[V(\mu\text{-}N)Cl_2(py)_2]_\infty$ (**2a**) showing the vanadium coordination sphere with 50% probability thermal ellipsoids for non-hydrogen atoms and the unit cell with 30% probability thermal ellipsoids for nonhydrogen atoms.

Table I. Selected Bond Distances (Å) and Angles (deg) for $[V(\mu\text{-}N)Cl_2(py)_2]_\infty$ (**2a**) and $V(N)Cl_2(quin)_2$ (**3c**)

	2a	**3c**
V–N(1)	1.571 (7)	1.568 (19)
V–N(2)	2.135 (6)	2.187 (17)
V–N(3)		2.236 (14)
V–Cl(1)	2.313 (2)	2.297 (6)
V–Cl(2)		2.267 (7)
V–N(1)′	2.729 (7)	5.78 (2)
N(1)–V–N(2)	96.9 (1)	94.8 (9)
N(1)–V–N(3)		95.0 (7)
N(2)–V–N(3)	166.2 (2)	170.2 (6)
Cl(1)–V–Cl(2)	159.57 (11)	139.9 (3)
Cl(1)–V–N(1)	100.21 (6)	113.9 (6)
Cl(2)–V–N(1)		106.2 (7)
Cl(1)–V–N(2)	89.6 (2)	87.9 (5)
Cl(2)–V–N(2)		89.2 (4)
Cl(1)–V–N(3)	87.9 (2)	88.8 (4)
Cl(2)–V–N(3)		87.4 (4)

An X-ray structural study[13] reveals **2a** to be a linear chain polymer composed of six-coordinate vanadium atoms joined by alternating short (1.571 (7) Å) and long (2.729 (7) Å) vanadium–nitrogen bonds (Figure 1). The short V–N(1) distance is

---

(1) *Metal-Containing Polymeric Systems*; Sheats, J. E., Carraher, C. E., Jr., Pittman, C. U., Jr., Eds.; Plenum: New York, 1985. *Extended Linear Chain Compounds*; Miller, J. S., Ed.; Plenum: New York, 1982; Vol. 1–3. *Molecular Electronic Devices*; Carter, F. L., Ed.; Marcel Dekker: New York, 1982.

(2) Allcock, H. R. *Chem. Eng. News* **1985**, *63(11)*, 22–36.

(3) See, for example: Collman, J. P.; McDevitt, J. T.; Leidner, C. R.; Yee, G. T.; Torrance, J. B.; Little, W. A. *J. Am. Chem. Soc.* **1987**, *109*, 4606–4614. Hiller, W.; Strähle, J.; Datz, A.; Hanack, M.; Hatfield, W. E.; ter Harr, L. W.; Gütlich, P. *J. Am. Chem. Soc.* **1984**, *106*, 329–335. Williams, J. M. *Adv. Inorg. Chem. Radiochem.* **1983**, *26*, 235–268.

(4) Liese, W.; Dehnicke, K.; Walker, I.; Strähle, J. *Z. Naturforsch., B: Anorg. Chem., Org. Chem.* **1979**, *34B*, 693–696.

(5) (a) Chisholm, M. H.; Hoffman, D. M.; Huffman, J. C. *Inorg. Chem.* **1983**, *22*, 2903–2906. (b) Chan, D. M.-T.; Chisholm, M. H.; Folting, K.; Huffman, J. C.; Marchant, N. S. *Inorg. Chem.* **1986**, *25*, 4170–4174.

(6) Doherty, N. M.; Critchlow, S. C. *J. Am. Chem. Soc.* **1987**, *109*, 7906–7908.

(7) Chan, D.M.-T., DuPont, personal communication. Becker, F. *J. Organomet. Chem.* **1973**, *51*, C9–C10. Shihada, A.-F. *Z. Anorg. Allg. Chem.* **1974**, *408*, 9–14.

(8) Ligand redistribution between tetrahedral vanadium(V) centers is a common reaction. See, for example: Preuss, F.; Towae, W. *Z. Naturforsch., B: Anorg. Chem., Org. Chem.* **1981**, *36B*, 1130–1135.

(9) Schweda, E.; Scherfise, K. D.; Dehnicke, K. *Z. Anorg. Allg. Chem.* **1985**, *528*, 117–124.

(10) Griffith, W. P. *Coord. Chem. Rev.* **1972**, *8*, 369–396. Dehnicke, K.; Strähle, J. *Angew. Chem., Int. Ed. Engl.* **1981**, *20*, 413–486.

(11) Nugent, W. A.; Haymore, B. L. *Coord. Chem. Rev.* **1980**, *31*, 123–175.

(12) Nakamoto, K. *Infrared and Raman Spectra of Inorganic and Coordination Compounds*, 4th ed.; Wiley: New York, 1986; p 206.

(13) After this work was submitted for publication, an independent crystallographic determination of the structure of **2a** (prepared by the thermal decomposition of $[V(N_3S_2)Cl(py)_2]_2$) appeared in press: Willing, W.; Christophersen, R.; Müller, U.; Dehnicke, K. *Z. Anorg. Allg. Chem.* **1987**, *555*, 16–22.

indicative of a strong vanadium–nitrogen triple bond,[14] whereas the very long V–N(1) bond is best described as a weak dative interaction since it is significantly longer that the sum of the covalent radii (1.92 Å according to Pauling[15]). Compare also the V–N distance of 2.135 (6) Å for the coordinated pyridine ligand in **2a**. This leads to an overall description of the nitride bridge as V≡N:→V. The chloride and pyridine ligands coordinated to each vanadium bend away from the vanadium–nitrogen multiple bond (Table I). The distorted octahedral geometry about the vanadium(V) center is similar to that observed for almost all six-coordinate imido and nitrido complexes[10,11] and consistent with the strong trans influence expected for multiply bonded ligands, especially at d^0 metal centers.[11] The unit cell of **2a** contains four symmetry-related $[V(N)Cl_2(py)_2]$ fragments incorporated into two neighboring chains which point in opposite directions. The chloride and pyridine ligands are in alternating positions along the VN chain which lies on the 2-fold axis (Figure 1). Each pyridine ring is twisted from the plane containing the VN axis and the pyridine nitrogen by a dihedral angle of 39.3°. The symmetry-related pyridine ligands on adjacent chains are parallel and overlap such that the planes of the two pyridine rings are separated by 3.48 Å, a suitable distance for van der Waals interaction of their π-systems.[15]

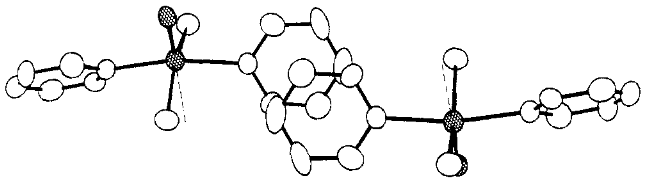

An analogous insoluble red crystalline compound is obtained on reaction of **1** with 4-methylpyridine (**2b**) (eq 2). In contrast, however, **1** reacts with 4-ethylpyridine or 4-*tert*-butylpyridine to produce *soluble* vanadium nitride derivatives of formula $V(N)Cl_2L_2$ (**3**) (eq 3). A soluble nitride complex (**3c**) is also prepared

$$\underset{\mathbf{1}}{Cl_3V{\equiv}NSiMe_3} + 2L \xrightarrow{-ClSiMe_3} \underset{\substack{\mathbf{3a},\ L = 4\text{-Etpy} \\ \mathbf{3b},\ L = 4\text{-}t\text{-Bupy} \\ \mathbf{3c},\ L = \text{quin}}}{Cl_2L_2V{\equiv}N:} \qquad (3)$$

on reaction of **1** with an aliphatic amine, quinuclidine (1-azabicyclo[2.2.2]octane) (eq 3). These reactions are quantitative by ^{1}H NMR. Compounds **3a–c** are isolated as red crystalline solids and are characterized by ^{1}H, ^{13}C, and ^{51}V NMR spectroscopies, IR spectroscopy, and elemental analysis.

A molecular weight determination for **3b** supports a monomeric formulation for the soluble nitride compounds in solution.[16] An X-ray structural study indicates that **3c** is monomeric in the solid state as well. The five ligands coordinated to the vanadium in **3c** define a distorted trigonal bipyramidal geometry with the quinuclidine ligands in approximately axial sites (N(2)–V–N(3) = 170.2 (6)°) (Figure 2). The quinuclidine α-carbons are staggered relative to the vanadium–nitride bond. The angles between the equatorial ligands (Table I) indicate distortion toward the square-pyramidal structure which is more common for five-coordinate nitrido complexes.[10,11] The V–N(1) distance of 1.568 (19) Å is again short[14] and indicates a strong vanadium–nitrogen triple bond. A unit cell drawing of **3c** (Figure 2) shows the absence of the briding-nitride interaction; the closest intermolecular distance from N(1) to V is 5.78 (2) Å.

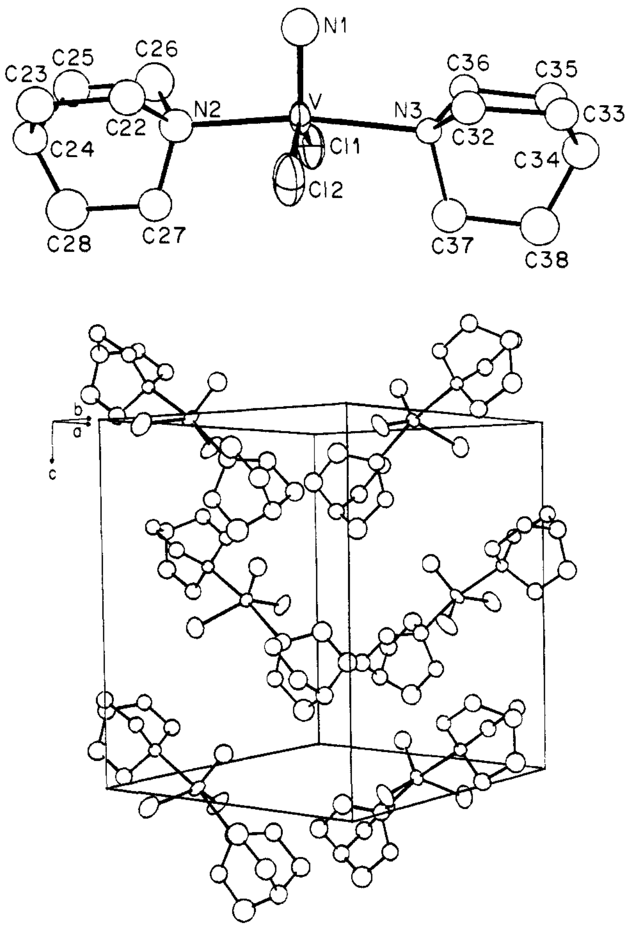

Figure 2. ORTEP drawings of $V(N)Cl_2(quin)_2$ (**3c**) showing the individual molecule and the unit cell with 30% probability thermal ellipsoids for non-hydrogen atoms.

Discussion

A series of vanadium(V) nitrido complexes of formula $[V(N)Cl_2L_2]_n$ has been prepared by net loss of chlorotrimethylsilane from the vanadium(V) trimethylsilylimido trichloride (**1**) on addition of substituted pyridine or amine ligands. Compounds **2** and **3** are rare examples of vanadium nitride derivatives;[17] furthermore, **2a** and **3c** are the only structurally characterized examples of vanadium nitride compounds[13] and possess the shortest vanadium–nitrogen bonds known.

Depending on the identity of the ancillary ligands, $[V(N)Cl_2L_2]_n$ adopts either a polymeric nitride-bridged linear chain structure or a monomeric terminal nitrido structure. This results in a striking difference in solubility between the two sets of compounds. The insolubility of **2a** suggests that it possesses a very stable linear chain structure. The long V–N(1) bridge bond distance, however, implies that the nitride bridge is extremely weak. This indicates that some other factor in the solid-state structure of **2a** is important in stabilizing the polymeric chain. We propose that the interchain pyridine interaction observed for **2a** is crucial to the stability of the solid-state polymer. This then explains the variation in solubility and structure on changing the para substituent of the pyridine ligand. Compound **2b** with a 4-methyl group can adopt a structure analogous to **2a** and, therefore, is insoluble; however, the 4-ethyl and 4-*tert*-butyl substituents in **3a,b** are sufficiently bulky to prevent stabilizing overlap of the pyridine ligands on neighboring chains, producing soluble monomeric derivatives. Likewise, **3c** has no aromatic ring to engage in the stabilizing π-interaction and thus favors a terminal nitrido structure.

Use of the condensation reaction to produce **2** or **3** results in a weak or nonexistent nitride bridge, in contrast to the robust nitride bridge we have observed for the heterobimetallic complex $(Me_3SiO)_3V{\equiv}N{-}Pt(Me)(PEt_3)_2$.[6] The very short V–N multiple bonds observed for **2a** and **3c** suggest an explanation for the

---

[14] (a) Vanadium(V)–nitrogen triple bond distances range from 1.59 (1) Å for **1**[9] to 1.688 (6) Å for $Cl_3(bipy)V{\equiv}NCl$.[14b] (b) Lörcher, K.-P.; Strähle, J.; Walker, I. *Z. Anorg. Allg. Chem.* **1979**, *452*, 123–140.

[15] Pauling, L. *The Nature of the Chemical Bond*, 3rd ed.; Cornell University Press: Ithaca, NY, 1960; Chapter 7.

[16] Compounds **3a** and **3c** are not sufficiently stable in solution over long periods of time to allow determination of their solution molecular weights.

[17] Scherfise, K. D.; Dehnicke, K. *Z. Anorg. Allg. Chem.* **1986**, *538*, 119–122. Goedken, V. L.; Ladd, J. A. *J. Chem. Soc., Chem. Commun.* **1981**, 910–911.

weak/nonexistent nitride bridges in this system. Vanadium is a transition element which, in its high oxidation states, forms strong interactions with multiply bonding ligands such as oxo and imido; for example, the vanadyl and vanadate ions are ubiquitous in aqueous vanadium chemistry,[18] and a variety of vanadium(V) organoimido complexes are known.[11] Qualitatively, this suggests that in a polymeric system formation of a short, strong triple bond between the nitrogen atom and one vanadium(V) center might be more favorable than two longer, weaker double bonds in V=N=V. The trans labilizing influence of the triply bonded nitride ligand[11] would explain the weak dative nitride bridge.

Wheeler, Hoffmann, et al. have examined the electronic structure of linear chain nitride-bridged systems,[19] and their calculations support this qualitative picture. Their studies indicate that, in general, π-bonding in μ_2-X linear chains (X = N, O, or halide) will favor an asymmetric structure and will dominate over the σ-bonding preference for a symmetric ligand bridge.[19] The asymmetric structure in **2a** can be viewed as arising from a second-order Peierls distortion of the metal–nitride π-bonding, closely related to the bond-alternated structure of polyacetylene.[19,20]

In general, nitride-bridged compounds can adopt a range of μ_2 structures, from the very asymmetric bridge observed for **2a** ($M{\equiv}N{:}{\rightarrow}N$) to the symmetric bridge (M=N=M) observed for several homobimetallic μ-nitrides.[21] However, only asymmetric structures have been observed for the known polymeric metal nitrides: $Re(N)Cl_4$,[4] $W(N)(O\text{-}t\text{-}Bu)_3$,[5a] $Mo(N)(OR)_3$ (R = *t*-Bu, *i*-Pr),[5b] and **2a**. In spite of its very weak nitride bridge, the polymeric structure in **2a** is more stable than that in $Re(N)Cl_4$ or $M(N)(OR)_3$ (M = Mo or W). The rhenium–nitride linear chain is readily disrupted by added ligands,[4] and the molybdenum and tungsten compounds are monomers in benzene solution at ambient temperatures;[5] in contrast, decomposition of **2a** requires heating at 120 °C in pyridine solvent. This further supports the idea that the interchain pyridine interaction imparts a significant stabilization to the structure of **2a**. The next question to address in this system is how formation of this very stable solid-state polymeric structure occurs. We are currently exploring the mechanism of the condensation/polymerization reaction in order to understand this process and to apply this chemistry to the synthesis of a variety of new transition-metal-containing polymers.

Conclusions

We have succeeded in using the condensation reaction in eq 1 for formation of polymeric metallonitrides. Surprisingly however, the overall stability of the nitride-bridged structure in $[V(N)Cl_2L_2]_n$ is not dependent on the $V(\mu\text{-}N)V$ chain bonding but rather on the identity of the coordinated ligands and the interactions between these ligands in the solid state.

Experimental Section

General Considerations. All manipulations were performed in a nitrogen atmosphere with glovebox, Schlenk, or vacuum-line techniques. Solvents and pyridine were dried over activated 4-Å molecular sieves, stored over CaH_2, and vacuum transferred prior to use. NMR solvents were dried over activated 4-Å molecular sieves. Vanadium(V) oxychloride was purchased from Strem and used as received. Chan's modification of a literature method was used to prepare $(Me_3SiO)_3V(NSiMe_3)$.[7] Substituted pyridines (Aldrich) were purified by distillation under N_2; quinuclidine (Aldrich) was purified by vacuum sublimation. NMR spectra were recorded on Varian VXL300 (299.95 MHz ^{1}H, 78.86 MHz ^{51}V, 75.43 MHz ^{13}C) and Bruker WM500 (500.14 MHz ^{1}H) spectrometers in benzene-d_6 at ambient temperatures; chemical shifts are reported in ppm downfield from $SiMe_4$ (^{1}H and ^{13}C NMR) or $VOCl_3$ (^{51}V NMR). IR spectra were obtained as Nujol mulls with Perkin-Elmer 283 and 1600 spectrometers. Elemental analyses were performed by Canadian Microanalytical Services, Ltd. Solution molecular weights were determined by the Signer method.[22]

Procedures. $Cl_3V(NSiMe_3)$[9] (1). A solution of $VOCl_3$ (13.0 mL, 138 mmol) in hexane (10 mL) was added to a solution of $(Me_3SiO)_3V(NSiMe_3)$ (16.0 g, 39.4 mmol) in pentane (100 mL) at −78 °C. Stirring for 30 min at −78 °C resulted in precipitation of orange **1**. While at −78 °C, the solid was allowed to settle, and the supernatant liquid was removed by syringe; the solid was washed with pentane at −78 °C (2 × 25 mL) by the same procedure. The cooling bath was removed from the reaction flask, and any remaining solvent was removed under reduced pressure as the reaction mixture warmed to 0 °C, resulting in a dark orange solid which converts to a black oil on standing at ambient temperature. Kugelrohr sublimation of the crude product at 30 °C to a receiving flask cooled to 0 °C yields 3.66 g (38%) of orange crystalline **1**. Further purification can be effected by recrystallization from pentane or resublimation: ^{1}H NMR −0.09 (s); ^{51}V NMR 10.5 (s, $\nu_{1/2}$ = 230 Hz).

$[V(\mu\text{-}N)Cl_2(py)_2]_\infty$ (2a). Pyridine (70 μL, 0.87 mmol) was added to a frozen (−78 °C) benzene solution of freshly recrystallized **1** (0.10 g, 0.41 mmol). The mixture was allowed to warm to 22 °C; on melting, the orange solution turned red and a pink solid immediately precipitated. The solid was collected by filtration and washed with benzene (3 × 5 mL) producing 0.12 g of microcrystalline **2a** (100%): IR 3148 br, 3115, 3074, 3052, 3030, 1607 s, 1572, 1538, 1486, 1449, 1409, 1240, 1220, 1158, 1073, 1046, 1016, 968 s ($\nu_{V\equiv N}$), 942, 877, 844, 763 s, 722, 693/689 s, 645, 608 cm^{-1}. Anal. Calcd for $C_{10}H_{10}Cl_2N_3V$: C, 40.85; H, 3.43; N, 14.29. Found: C, 40.65; H, 3.40; N, 13.94.

$[V(\mu\text{-}N)Cl_2(4\text{-}Mepy)_2]_\infty$ (2b). The above procedure was followed with 0.19 g (0.70 mmol) of **1** and 0.14 mL (1.44 mmol) of 4-methylpyridine, yielding 0.19 g of pink microcrystalline **2b** (85%): IR 3138 br, 3048, 1619 s, 1559, 1503, 1410, 1337, 1211, 1068, 1032, 950 s ($\nu_{V\equiv N}$), 865, 814, 720, 559, 497 s cm^{-1}. Anal. Calcd for $C_{12}H_{14}Cl_2N_3V$: C, 44.77; H, 4.38; N, 13.04. Found: C, 44.73; H, 4.48; N, 12.68.

$V(N)Cl_2(4\text{-}Etpy)_2$ (3a). (a) A sample of **1** (10 mg, 0.04 mmol) in an NMR tube equipped with a Teflon value adapter was dissolved in benzene-d_6 (0.4 mL). The orange solution was frozen to −78 °C, 4-ethylpyridine (10 μL, 0.09 mmol) was added, and the tube was sealed. Warming to 22 °C immediately produced a deep red solution with ^{1}H NMR signals characteristic of **3a** plus 1 equiv of $ClSiMe_3$. However, attempts to prepare **3a** by reaction of **1** and 4-ethylpyridine in benzene produced an impure oily red sample. (b) A solution of **1** (0.31 g, 1.3 mmol) in pentane (10 mL) was filtered to remove a small amount of dark insoluble material into a solution of 4-ethylpyridine (0.30 mL, 2.6 mmol) in pentane (10 mL) resulting in immediate formation of a mustard yellow precipitate. The solvent was removed under reduced pressure, and the yellow solid was dissolved in benzene to produce a red solution. The volume was reduced to 5 mL resulting in crystallization of pink **3a** which was collected by filtration and washed with benzene (3 × 3 mL) yielding 0.18 g (42%): ^{1}H NMR 9.10 (d, *J* = 6 Hz), 6.35 (d, *J* = 6 Hz), 1.85 (q, *J* = 8 Hz), 0.63 (t, *J* = 8 Hz); ^{51}V NMR −65.2 (s, $\nu_{1/2}$ = 700 Hz); ^{13}C{^{1}H} NMR 156.7, 151.7, 123.9, 28.1, 13.4; IR 3128, 3093, 3073/3066, 3048, 1696, 1619 s, 1552, 1502, 1429, 1350, 1230, 1206, 1112, 1063, 1032, 1009 s, 986, 978, 866, 830 s, 796, 733/722, 580 s, 516 cm^{-1}. Anal. Calcd for $C_{14}H_{18}Cl_2N_3V$: C, 48.02; H, 5.18; N, 12.00. Found: C, 47.74; H, 5.19; N, 11.76.

$V(N)Cl_2(4\text{-}t\text{-}Bupy)_2$ (3b). A sample of **1** (0.25 g, 1.0 mmol) was dissolved in benzene (10 mL) and filtered to remove a small amount of dark insoluble material. A solution of 4-*tert*-butylpyridine (0.20 mL, 2.0 mmol) in benzene (15 mL) was added, and the mixture was stirred for 30 min producing a deep red solution. The solvent volume was reduced to 5 mL producing pink crystalline **3b** which was collected by filtration and dried in vacuum (0.23 g, 55%): ^{1}H NMR 9.19 (d, *J* = 6 Hz), 6.66 (d, *J* = 6 Hz), 0.79 (s); ^{51}V NMR −63.5 (s, $\nu_{1/2}$ = 880 Hz); ^{13}C{^{1}H} NMR 163.5, 152.0, 121.6, 34.9, 29.9; IR 3144 br, 1614 s, 1544, 1500, 1422, 1274, 1228, 1203, 1072, 1039, 1027, 1007, 976, 937, 844, 833 s, 730, 571 s, 550 cm^{-1}; mol wt (C_6H_6) calcd 406, found 420 ± 22. Anal. Calcd for $C_{18}H_{26}Cl_2N_3V$: C, 53.22; H, 6.45; N, 10.34. Found: C, 53.45; H, 6.68; N, 10.17.

$V(N)Cl_2(quin)_2$ (3c). The above procedure was followed with 0.25 g (1.0 mmol) of **1** and 0.24 g (2.2 mmol) of quinuclidine, yielding 0.30 g of dark pink crystalline **3c** (82%): ^{1}H NMR 3.77 (t, *J* = 8 Hz), 1.26 (septet, *J* = 3 Hz), 1.19 (m); ^{51}V NMR 63.6 (s, $\nu_{1/2}$ = 550 Hz); ^{13}C{^{1}H} NMR 53.4, 26.7, 20.7; IR 1483, 1349, 1314, 1278, 1201, 1115, 1033 s, 1022, 1000, 979, 970, 833, 814, 781/775, 722, 675, 631 cm^{-1}. Anal.

---

(18) Cotton, F. A.; Wilkinson, G. *Advanced Inorganic Chemistry*, 4th ed.; Wiley: New York, 1980; pp 710–716.

(19) Wheeler, R. A.; Whangbo, M.-H.; Hughbanks, T.; Hoffmann, R.; Burdett, J. K.; Albright, T. A. *J. Am. Chem. Soc.* **1986**, *108*, 2222–2236. Wheeler, R. A.; Hoffmann, R.; Strähle, J. *J. Am. Chem. Soc.* **1986**, *108*, 5381–5387.

(20) Critchlow, S. C.; Smith, R. C.; Doherty, N. M. In *Atomic and Molecular Processing of Electronic and Ceramic Materials: Preparation, Characterization, and Properties*; Aksay, I. A., McVay, G. L., Stoebe, T. G., Wager, J. F., Eds.; Materials Research Society: Pittsburgh, PA, 1988; pp 153–158.

(21) Hörner, M.; Frank, K.-P.; Strähle, J. *Z. Naturforsch., B: Anorg. Chem., Org. Chem.* **1986**, *41B*, 423–428, and references therein. Griffith, W. P.; McManus, N. T.; Skapski, A. C. *J. Chem. Soc., Chem. Commun.* **1984**, 434–435, and references therein.

(22) Clark, E. P. *Ind. Eng. Chem., Anal. Ed.* **1941**, *13*, 820–821.

Table II. Positional and Equivalent Isotropic Thermal Parameters[a] for $[V(\mu\text{-}N)Cl_2(py)_2]_\infty$ (**2a**)

atom	x	y	z	B (Å^2)
V	0.250	0.750	0.4975 (2)	2.73 (3)
Cl	0.13114 (12)	0.6006 (2)	0.4498 (2)	3.26 (4)
N(1)	0.250	0.750	0.6802 (8)	2.7 (2)
N(2)	0.3328 (3)	0.5656 (6)	0.4677 (6)	2.8 (1)
C(1)	0.3922 (5)	0.5544 (9)	0.3540 (8)	2.9 (2)
C(2)	0.4429 (5)	0.4321 (11)	0.3303 (9)	4.4 (2)
C(3)	0.4308 (5)	0.3152 (10)	0.4250 (10)	4.9 (2)
C(4)	0.3687 (6)	0.3233 (9)	0.5436 (9)	4.8 (2)
C(5)	0.3224 (5)	0.4503 (9)	0.5601 (9)	4.1 (2)

[a] Anisotropically refined atoms are given in the form of the isotropic equivalent thermal parameter defined as $^4/_3[a^2\beta_{11} + b^2\beta_{22} + c^2\beta_{33} + ab(\cos\gamma)\beta_{12} + ac(\cos\beta)\beta_{13} + bc(\cos\alpha)\beta_{23}]$.

Calcd for $C_{14}H_{26}Cl_2N_3V$: C, 46.94; H, 7.32; N, 11.73. Found: C, 47.54; H, 7.20; N, 11.43.

Structure Determination for $[V(\mu\text{-}N)Cl_2(py)_2]_\infty$ (2a). Crystals of **2a** were obtained in the following manner: Pyridine (15 mL) was vacuum transferred into a glass tube containing **1** (0.12 g, 0.49 mmol) at −78 °C, and the tube was sealed. Pink **2a**, which precipitated on warming to ambient temperature, was dissolved by immersing the glass tube in an oil bath at 120 °C for 1 min producing a red solution. The mixture was allowed to cool to ambient temperature resulting in the formation of long, thin needle-shaped red crystals of **2a**.

A suitable single crystal of dimensions 0.27 × 0.060 × 0.035 mm was mounted in a glass capillary under N_2; although a weak diffractor due to its small size, the crystal gave very sharp diffraction peaks. Intensity data were obtained at 25 °C on an Enraf-Nonius CAD4 diffractometer with Mo Kα radiation monochromatized with graphite ($\lambda = 0.71037$ Å). All data reduction and computations were performed with the SDP/VAX program package supplied by Enraf-Nonius Corp. A total of 4875 reflections with $2\theta \leq 50°$ in the four octants $hk\bar{l}$, $h\bar{k}\bar{l}$, $\bar{h}k\bar{l}$, and $\bar{h}\bar{k}\bar{l}$ were collected with the θ–2θ scan technique with a scan range $\Delta\theta = 0.85° + 0.347 \tan\theta$ and a scan rate of $\simeq 0.8°$ min^{-1}. The systematic extinctions were appropriate for the space group *Pccn*. The data were corrected for decay (linear, according to the 13.9% decrease in intensity of three standard reflections with $2\theta \simeq 26°$ measured roughly every 60 reflections) and for Lorentz, polarization, and absorption effects (an empirical correction based on a set of ϕ scans, $\mu = 12.1$ cm^{-1}; transmission coefficients ranged from 0.999 to 0.866, av = 0.930). Averaging in the space group *Pccn* yielded 1262 reflections; the final data set consisted of 388 unique observed reflections with $I > 2\sigma_I$ ($R_{av} = 0.072$). Precise unit cell dimensions, $a = 15.229$ (2) Å, $b = 9.245$ (1) Å, $c = 8.599$ (1) Å, $V = 1210.7$ (5) Å^3, with $Z = 4$, $D_{calcd} = 1.615$ g/cm^3, were obtained from a least-squares fit of the setting angles of 25 reflections with $23° < 2\theta < 31°$ which were centered on both Friedel-related peaks ($\pm 2\theta$).

The vanadium and chlorine atoms were located on a Patterson map, and the structure was solved by subsequent least-squares refinements and Fourier syntheses. The hydrogen atoms on the pyridine rings were fixed in calculated positions which were confirmed by a difference map. Final refinement with all nine independent non-hydrogen atoms anisotropic (74 parameters) converged at $R = 0.038 = \Sigma||F_o| - |F_c||$ and $R_w = 0.036 = [\Sigma w(|F_o| - |F_c|)^2/\sum wF_o{}^2]^{21/2}$ where $w = 1/(\sigma_F)^2$ with a ρ value of 0.04 used to downweight intense reflections;[23] GOF = 0.70, highest final residual electron density = ±0.5 e/Å^3. Scattering factors and anomalous dispersion terms were taken from the standard compilations.[24] Selected bond distances and angles are listed in Table I; positional and equivalent isotropic thermal parameters for non-hydrogen atoms are in Table II.

Table III. Positional and Equivalent Isotropic Thermal Parameters for $V(N)Cl_2(quin)_2$ (**3c**)

atom	x	y	z	B (Å^2)
V	0.1345 (3)	0.2584 (3)	0.000	3.46 (6)[a]
Cl(1)	−0.0507 (4)	0.2441 (6)	0.0239 (5)	5.8 (1)[a]
Cl(2)	0.2917 (5)	0.1867 (6)	0.0716 (6)	6.7 (2)[a]
N(1)	0.1686 (13)	0.3424 (17)	−0.0953 (15)	5.4 (5)
N(2)	0.1348 (14)	0.4122 (15)	0.1132 (13)	4.6 (4)
N(3)	0.1280 (12)	0.0804 (13)	−0.0920 (12)	2.6 (3)
C(22)	0.243 (2)	0.475 (2)	0.118 (2)	4.8 (6)
C(23)	0.248 (2)	0.581 (2)	0.200 (2)	5.3 (6)
C(24)	0.140 (2)	0.591 (2)	0.251 (2)	4.7 (6)
C(25)	0.058 (2)	0.617 (2)	0.167 (2)	5.9 (6)
C(26)	0.054 (2)	0.509 (2)	0.087 (2)	6.5 (6)
C(27)	0.118 (2)	0.363 (2)	0.219 (2)	4.4 (5)
C(28)	0.109 (2)	0.476 (2)	0.301 (2)	7.3 (8)
C(32)	0.233 (2)	0.046 (2)	−0.142 (2)	4.2 (5)
C(33)	0.224 (2)	−0.072 (2)	−0.207 (2)	3.8 (5)
C(34)	0.116 (2)	−0.129 (2)	−0.194 (2)	5.1 (6)
C(35)	0.032 (2)	−0.038 (2)	−0.237 (2)	4.3 (6)
C(36)	0.047 (2)	0.086 (2)	−0.174 (2)	3.4 (5)
C(37)	0.094 (2)	−0.027 (2)	−0.018 (2)	4.6 (6)
C(38)	0.094 (2)	−0.151 (2)	−0.080 (2)	5.8 (7)

[a] Atoms were refined anisotropically and are given in the form of the isotropic equivalent thermal parameter defined as $^4/_3[a^2\beta_{11} + b^2\beta_{22} + c^2\beta_{33} + ab(\cos\gamma)\beta_{12} + ac(\cos\beta)\beta_{13} + bc(\cos\alpha)\beta_{23}]$.

Structure Determination for $V(N)Cl_2(quin)_2$ (3c). Red crystals of **2a** were grown by slow evaporation of solvent from a benzene solution at 22 °C over 3 weeks. A crystal of dimensions 0.40 × 0.08 × 0.06 mm was mounted in a glass capillary under N_2. Data collection, processing, and structure solution were performed as above except as indicated. A total of 3376 reflections with $2\theta \leq 50°$ in the two octants $hk\bar{l}$, $\bar{h}\bar{k}l$ were collected with a scan rate of 1.2° min^{-1}. The systematic absences together with volume considerations indicated the acentric space group $Pca2_1$. There was a 19.3% decay in intensity based on three reflections $17° < 2\theta < 20°$ measured roughly every 100 reflections. No absorption correction was deemed necessary ($\mu = 8.92$ cm^{-1}). Averaging in the space group $Pca2_1$ yielded 1709 reflections; the final data set consisted of 605 unique observed reflections with $I > 2\sigma_I$ ($R_{av} = 0.062$). Precise unit cell dimensions, $a = 12.263$ (2) Å, $b = 10.675$ (2) Å, $c = 12.764$ (3) Å, $V = 1670.9$ (9) Å^3, with $Z = 4$, $D_{calcd} = 1.424$ g/cm^3, were obtained with 22 reflections with $23° < 2\theta < 28°$. The initial model from a Patterson map included the vanadium, one chlorine, and the two quinuclidine nitrogen atoms; the structure was solved by conventional methods. Final refinement with only the vanadium and chlorine atoms anisotropic and with calculated hydrogen atoms (95 parameters) yielded $R = 0.081$ and $R_w = 0.077$; GOF = 1.33, residual electron density = ±0.6 e/Å^3. The alternate enantiomorph consistently refined to marginally higher residuals and goodness of fit. Selected bond distances and angles are listed in Table I; positional and equivalent isotropic thermal parameters for non-hydrogen atoms are in Table III.

Acknowledgment. Support of this work by the donors of the Petroleum Research Fund, administered by the American Chemical Society; by the IBM Corporation; and by the Air Force Office of Scientific Research, Air Force Systems Command, USAF, Grant no. AFOSR-87-0362 is gratefully acknowledged. We also acknowledge support of X-ray equipment from the National Science Foundation (CHE-8617965) and the Graduate School Research Fund of the University of Washington (PHS Grant RR-0796).

Supplementary Material Available: Crystallographic data for **2a** and **3c**: anisotropic thermal parameters, hydrogen atom coordinates, bond distances and angles, torsional angles, and least-squares planes (7 pages); tables of observed and calculated structure factors (5 pages). Ordering information is given on any current masthead page.

---

(23) Corfield, P. W. R.; Doedens, R. J.; Ibers, J. A. *Inorg. Chem.* **1967**, *6*, 197–204.

(24) *International Tables of X-ray Crystallography*; Kynoch: Birmingham, England, 1974; Vol. IV.